Published in final edited form as:
J Biol Rhythms. 2012 October ; 27(5): 353–364. doi:10.1177/0748730412455918.

A mechanism for circadian control of pacemaker neuron excitability

Marc Ruben, **Mark D. Drapeau**[2], **Dogukan Mizrak**, and **Justin Blau**[1]
Department of Biology, New York University, 100 Washington Square East, New York, NY 10003, USA

Abstract

Although the intracellular molecular clocks that regulate circadian (~24 hr) behavioral rhythms are well-understood, it remains unclear how molecular clock information is transduced into rhythmic neuronal activity that in turn drives behavioral rhythms. To identify potential clock outputs, we generated expression profiles from a homogeneous population of purified pacemaker neurons (LN_vs) from wild type and clock mutant *Drosophila*. We identified a group of genes with enriched expression in LN_vs and a second group of genes rhythmically expressed in LN_vs in a clock-dependent manner. Only 10 genes fell into both groups: four core clock genes including *period* and *timeless*, and six genes previously unstudied in circadian rhythms. We focused on one of these six genes, *Ir*, which encodes an Inward rectifier K^+ channel likely to regulate resting membrane potential and whose expression peaks around dusk. Reducing *Ir* expression in LN_vs increased larval light avoidance and lengthened the period of adult locomotor rhythms, consistent with increased LN_v excitability. In contrast, increased *Ir* expression made adult flies largely arrhythmic and strongly dampened Period protein oscillations. We propose that rhythmic *Ir* expression contributes to daily rhythms in LN_v neuronal activity, which in turn feed back to regulate molecular clock oscillations.

Keywords

Circadian rhythm; *Drosophila*; Pacemaker neuron; Circadian transcription; Expression profiling; Inward rectifier channel

Introduction

Forward genetic screens in mice and *Drosophila* have revealed a conserved mechanism for the molecular clocks that operate in key central brain pacemaker neurons to generate circadian (~24hr) rhythms in behavior and physiology. These molecular clocks consist of interlocked transcriptional-translational feedback loops that drive circadian rhythms in gene expression (reviewed by Hardin, 2011).

At the cellular level, circadian pacemaker neurons show electrical activity rhythms (Michel et al., 1993; Welsh et al., 1995; Cao and Nitabach, 2008; Sheeba et al., 2008). Electrical

[1]Corresponding author: justin.blau@nyu.edu.
[2]Current address: Microsoft Corp., 5404 Wisconsin Ave., Chevy Chase, MD 20815

activity rhythms are presumably regulated by the molecular clock since the period of the firing rate of mammalian pacemaker neurons in the Suprachiasmatic nucleus (SCN) is altered in clock mutants with non-24hr rhythms (Liu et al., 1997; Herzog et al., 1998). However, direct links between the molecular clock and neuronal activity have proved elusive even though a number of channels and currents have been implicated in controlling pacemaker neuron activity,

For example, SCN firing frequency rhythms are likely regulated by BK/Kcnma1, a Ca^{2+}-activated K^+ channel, and by the Kv3.1/Kcnc1 and Kv3.2/Kcnc2 fast-delayed rectifier K^+ channels (Itri et al., 2005; Meredith et al., 2006; Kudo et al., 2011). *BK* RNA levels are rhythmic in the SCN (Panda et al., 2002). Kv3.1 and 3.2 protein levels are also rhythmic (Itri et al., 2005), although the mechanism underlying this has not been established. Mice lacking either BK or both Kv3.1 and Kv3.2 display weakened behavioral rhythms although no altered periods were seen (Meredith et al., 2006; Kudo et al., 2011). However, BK rhythms appear to be widespread and uniformly phased throughout the SCN (Meredith et al., 2006), making it difficult to explain how BK could account for regional differences in firing phase (Jagota et al., 2000; Saeb-Parsy and Dyball, 2003). Recent studies in mammals indicate that the SK channel may be more important than BK in the subgroup of Per+ SCN neurons that show dramatic daily changes in their resting membrane potential (Belle et al., 2009). Indeed, diversity in clock neurons across the SCN may have obscured the identification of specific clock-regulated outputs. To avoid these issues, we decided to generate whole genome expression profiles from a single defined group of pacemaker neurons.

We chose to study the ventral Lateral Neurons (LN_Vs) from *Drosophila*. The adult small LN_Vs (s-LN_Vs) are the master circadian pacemaker neurons and set the pace for other fly clock neurons and for locomotor activity rhythms (Stoleru et al., 2005). However, we purified LN_vs from larval brains for three main reasons: (1) The four larval LN_vs in each brain lobe are differentiated neurons with functional molecular clocks and become the adult s-LN_vs. (2) Larval LN_vs modulate circadian rhythms in light avoidance, which peaks at dawn (Mazzoni et al., 2005; Collins et al., 2012) just as s-LN_vs drive morning activity in adult flies (Grima et al., 2004; Stoleru et al., 2004), suggesting that larval LN_vs are functionally similar to adult s-LN_vs. (3) The neuropeptide Pigment Dispersing Factor (PDF) distinguishes LN_vs from other clock neurons. However, in adult flies, PDF is also produced in the large LN_vs (l-LN_vs) which regulate sleep rather than circadian rhythms (Parisky et al., 2008; Shang et al., 2008; Sheeba et al., 2008; Chung et al., 2009). Thus using *Pdf-Gal4* to mark larval LN_vs, we purified a homogeneous population of circadian pacemaker neurons for whole genome expression profiling, with the idea that genes expressed in larval LN_vs would also be expressed in the pacemaker adult s-LN_vs.

Materials and Methods

Isolation of larval neurons

For GeneChips, 3rd instar larvae were kept in a standard LD (Light:Dark) cycle and dissections centered around ZT3 or ZT15. [ZT: Zeitgeber time in a 12:12hr LD cycle. Lights on at ZT0, off at ZT12.] ~200 brains were dissected for each biological replicate, which took ~90 minutes. Thus cells were isolated from a narrow time range, rather than precisely at ZT3

or ZT15. For qPCR, larvae were taken from constant darkness and ~50 brains per replicate dissected. Dissected brains were transferred to Schneider's Insect Medium (Sigma) in non-stick tubes (Neptune) and kept on ice to minimize changes in gene expression. Brains were washed twice with cold PBS and dissociated as in Wegener et al. (2004) by transferring to a 50:50 mix of 1X Collagenase (Sigma): 1X Dispase II (Roche) and incubating for 2hr at 25°C. After 2hr, the dissociation solution was replaced with Schneider's medium with 10% Fetal Bovine Serum (FBS). Brains were then triturated 100x with a pipette and strained through a 35μm nylon mesh filter. Trypan Blue exclusion indicated that ~90% of larval LN_vs were viable after dissociation. Cells in Schneider's medium/10% FBS were kept on ice for transport to the NYU School of Medicine FACS center. To minimize contamination by cells attached to GFP+ or RFP+ cells, we used a size filter to remove cell clusters. Although Figure 1B shows a tail of cells with stronger GFP+ fluorescence than most, we only selected cells 2–3 orders of magnitude more fluorescent than most other cells. Cells were sorted directly into Arcturus PicoPure Total RNA extraction buffer. We analyzed RNA from 750 – 1,100 neurons for LN_v GeneChips, 1,000 or 10,000 GFP+ neurons for Elav GeneChips and 200–300 LN_vs for qPCR.

RNA amplification and analysis

For GeneChips, mRNA was amplified using the NuGen Ovation RNA Amplification System V2, and the resulting labeled single-stranded DNA hybridized to Affymetrix *Drosophila* 2.0 GeneChips. Hybridization, staining, and washing were as in the manufacturer's protocol. The entire procedure was performed 3 times each for each genotype (*Pdf-Gal4; UAS-CD8::GFP* larvae at ZT3 and ZT15 and per^0*; PDF-RFP* and *Pdf-RFP;* cyc^0 larvae at ZT15).

For Quantitative Real Time PCR (qPCR), we used an amplification strategy (WT-Ovation™ Pico System) optimized for smaller amounts of input total RNA than above to generate ~5μg of single stranded amplified unlabeled cDNA product. For each qPCR reaction, 20ng of cDNA was amplified in a Roche LightCycler. Forward and Reverse primers (F and R) and hybridization probes (P1 and P2) for quantitative PCR were designed so that one primer or probe spanned an exon/intron boundary to ensure that contaminating genomic DNA was either not amplified or measured. RNA levels were determined by comparing the time when the reaction moved into detectable exponential phase to standard curves for each primer set constructed by re-amplifying known quantities of PCR products. We normalized the absolute level of each gene in an experiment to RNA levels of *Pdf* (a non-cycling transcript) in that same experiment. qPCR results are an average of two or three independent experiments. For each time series plotted, the maximum value was set to 1, and other values are expressed as a fraction of the maximum. Primer sequences are in Supplementary Information.

GeneChip Data Analysis

Raw hybridization intensities from each CEL Affymetrix file (*Drosophila* 2.0 GeneChip) were analyzed using Matlab and accompanying bioinformatic toolbox. For the initial processing step, we used the gcrma algorithm (Irizarry et al., 2003) which incorporates a measure of nonspecific hybridization to compute an adjusted perfect match (aPM) intensity

for each probe. aPMs were then quantile-normalized (Irizarry et al., 2003) across replicates and experiments to yield a single expression measure for each probeset.

We removed low-intensity value probesets (lower 20th percentile)prior to testing for differential expression and a second filter removed probesets showing minimal-variance across all conditions (lower 20th percentile). Non-specific filtering when profiling homogenous tissue reduces noise introduced by the significant percentage of non-expressed and under-expressed genes, and thus improves sensitivity for detecting truly differentially-expressed genes (Blalock et al., 2003; Calza et al., 2007; Keegan et al., 2007).

Differential expression was determined using statistical analysis of variance (permuted Student's t-test) adjusted for multiple-hypothesis testing. To estimate false discovery rate, we followed the procedure introduced by (Storey and Tibshirani, 2003) to compute q-values and positive false discovery rate FDR (pFDR). We applied cutoffs for differentially-expressed genes of $p < .01$ and FDR < 8%. For genes meeting these statistical criteria, we further imposed fold change cutoffs: 8-fold for enrichment and 2-fold for time-dependence or clock-regulation. Correlations between the 3 replicates for each condition were as follows with numbers indicating highest and lowest correlations: ZT3 (0.92–0.88), ZT15 (0.91–0.88), *per^{0}* (0.95–0.92), *cyc^{0}* (0.94–0.87), Elav (0.89–0.87). Raw GeneChip data has been uploaded to GEO and is accessible via: http://www.ncbi.nlm.nih.gov/geo/query/acc.cgi?token=nbwdnouyqyquobg&acc=GSE35752

Fly stocks and Immunocytochemistry

The *Pdf-RFP* transgene has 0.6kb of *Pdf* regulatory genomic DNA (0.5kb upstream the start site of transcription and 0.1kb downstream) fused to DNA encoding mRFP1, a monomeric soluble red fluorescent protein (Shaner et al., 2004), generously provided by Roger Tsien. DNA was injected into *y w* flies by the MGH CBRC Transgenic *Drosophila* Core. We thank Ben Collins and Dave Reeves for these flies. Other fly strains are described in Supplementary Information. The P-element in *Ir^{d}* flies was excised using standard procedures. Immunodetection of whole-mount adult brains was as previously described using a monoclonal mouse antibody to PDF (Cyran et al., 2005), guinea-pig anti-VRI (generously provided by Paul Hardin), rabbit anti-GFP (Invitrogen) to detect nYFP and rabbit anti-PER (generously provided by Jeff Hall). PER levels were measured in 5 s-LN$_v$ clusters (each from a different brain) with typically 2–4 s-LN$_v$s per cluster in Figure 4.

Behavioral Analysis

To assay larval light avoidance, we followed the method of Mazzoni et al. (2005) in which 15 larvae roam for 15min on a 1% agar surface in a Petri-dish. We used a light box (developed by Alex Keene) with a fluorescent tube lighting the assay plate from below that is blocked from transmitting to half the Petri dish by non-translucent dividers placed between the light source and assay plates. Light intensity was reduced to 30lux by increasing the distance of the plates from the light source using these dividers and adding neutral transmittance filters (Roscolux #397: Pale Grey). Larvae on both sides were counted after 15min. Four plates were run in parallel, with each plate representing an individual experiment. Each data point is the mean of 12 plates.

For adult circadian assays, adult flies were placed in Trikinetics locomotor assay cuvettes and entrained to light-dark (LD) cycles for at least 3 days prior to shifting to constant darkness (DD) for at least 7 days. We calculated the period of each locomotor rhythm (τ), by chi-squared periodogram analysis as previously (Price et al., 1998). The power of the rhythm is the height in arbitrary units of the periodogram peak, which quantifies the rhythm strength and is only reported for flies meeting the significance threshold ($p < .01$). Visual inspection of actograms was also used to determine percent rhythmic flies in Figure 4.

Results

GeneChips identify transcripts enriched in larval LN_vs

To purify master pacemaker neurons, we dissected brains at ZT3 or ZT15 from larvae with the LN_v-specific driver, *Pdf-Gal4* (Park et al., 2000) expressing GFP (Figure 1A). Larval brains were dissociated into a single-cell suspension and flow cytometry used to select single GFP+ larval LN_vs. We typically obtained ~900 LN_vs from ~200 larval brains. mRNA was purified, amplified and the resulting labeled single-stranded DNA hybridized to GeneChips (Figure 1). We performed this procedure three times for each timepoint.

Before examining differences in gene expression in larval LN_vs between ZT3 and ZT15, we wanted to validate the procedure. We compared LN_v gene expression profiles with those from a heterogeneous group of larval brain neurons that produce the post-mitotic marker Elav. mRNAs whose expression was increased in LN_vs compared to Elav+ neurons were termed “enriched” (see Experimental Procedures). *Pdf* was the most highly enriched transcript in LN_vs: 610-fold more abundant at ZT15 in LN_vs than in Elav+ neurons (Figure 1 and Table 1a). The core clock genes *period* (*per*), *timeless* (*tim*), *vrille* (*vri*) and *PAR-domain protein 1* (*Pdp1*) were all in the top 130 enriched mRNAs at ZT15 (close to their peak expression time) with FDR < 8%, p-values (t-test) <0.01, and at least 8-fold enrichment. The inclusion of these genes validates the purity of the sample.

Applying these cutoffs, we identified 95 mRNAs enriched in LN_vs at ZT3, and 153 mRNAs at ZT15 (Table S1), with 57 mRNAs enriched at both time points. Several of the enriched mRNAs have known roles in LN_vs. In addition to *per*, *tim*, *vri* and *Pdp1* and the circadian photoreceptor *cryptochrome* (*cry*), the transcription factor Mef2 (53-fold enriched at ZT15) is produced in larval and adult LN_vs and regulates adult circadian rhythms (Blanchard et al., 2010). Thus the LN_v purification and RNA amplification method seems to work well.

An alternative strategy involving manual picking of *Drosophila* clock neurons was recently described (Nagoshi et al., 2010). We found 16 of the 63 LN_v-enriched mRNAs found by Nagoshi et al. (2010) in our ZT15-enriched datasets and these are underlined in Table S1. This overlap is considerably more than would be expected by chance and there are major differences between the two studies: Nagoshi et al. (2010) pooled data from larval and adult LN_vs (including l-LN_vs) and compared these data to a pooled reference sample of larval and adult Elav+ neurons as well as non-LN_v clock neurons. In addition, they isolated LN_vs at ZT12, 3hr earlier than our timepoint, and timing is very important in LN_vs: 61% (94/153) of the mRNAs we found enriched at ZT 15 were not enriched at ZT 3 (and see below for time-dependent LN_v expression).

GeneChips identify transcripts whose levels are time-dependent in LN_vs

CLK/CYC-regulated transcripts are low in larval LN_vs at ZT3 (early morning) and high at ZT15 (early evening). Therefore, we compared LN_v expression profiles at these time points to identify genes whose expression is time-dependent. As expected, expression of the core clock genes *per*, *tim*, *vri* and *Pdp1* was higher at ZT15 than ZT3 (Figure 1D, E and Table S2). We identified 195 mRNAs whose expression is 2-fold different in LN_vs between ZT3 and ZT15 applying the same statistical cutoffs for p-value and FDR as for enrichment (Table S2). 87% (161/195) of these mRNAs are not enriched transcripts and are presumably expressed broadly in the larval brain as well as in a time-dependent manner in LN_vs. Only 11 of the 195 time-dependent genes we identified in larval LN_vs (including *per*, *tim*, *vri*, and *Pdp1)* are among the rhythmic genes identified by meta-analyses of the multiple whole *Drosophila* head microarray studies (Wijnen et al., 2006; Keegan et al., 2007), validating the purification of LN_vs prior to GeneChip analysis. A recent study came to similar conclusions about rhythmic gene expression in adult LN_vs: Kula-Eversole et al. (2010) found that most rhythmically expressed genes in l-LN_vs do not show rhythmic expression in whole fly heads.

A subset of genes whose expression is time-dependent are clock-driven in LN_vs

Rhythmically expressed genes could be driven by LD cycles rather than by the molecular clock (Wijnen et al., 2006). To distinguish light-regulated from clock-regulated genes, we isolated LN_vs from *per* and *cyc* null mutants. These mutants have opposite effects on the molecular clock since PER protein represses CLK/CYC activity (reviewed by Hardin, 2011). Therefore, if any of the 195 time-dependent mRNAs are clock-regulated, their expression should differ between per^0 and cyc^0 larval LN_vs. Applying the same statistical cutoffs as for the ZT3 vs. ZT15 comparison, we identified 177 “clock-regulated” mRNAs whose expression differs between per^0 and cyc^0 LN_vs (Table S3 and Figure 1D). 24 mRNAs have both time-dependent (ZT3 vs. ZT15) and clock-regulated expression (per^0 vs. cyc^0), which we term “clock-driven” (Figure 1D–E). As expected, this group includes the known direct CLK/CYC target genes: *per*, *tim*, *vri* and *Pdp1*.

Two surprising omissions from the clock-driven list are *cry* and *Clk. cry* expression was more highly enriched at ZT3 than at ZT15, but did not meet the statistical cut-offs for time-dependency. This presumably reflects its delayed time to reach peak levels in larval LN_vs since, as described below, qPCR from isolated LN_vs revealed higher *cry* RNA levels at CT10 than CT4 in larval LN_vs. [CT: Circadian time: time in DD after prior LD cycles]. Thus our list of clock-driven LN_v transcripts is presumably incomplete for this reason and because other transcripts (such as *Clk*) are lowly expressed and/or difficult to amplify.

The lack of overlap between the genes showing time-dependent and clock-dependent expression is also surprising and remains to be fully explained. Interestingly, *per*, *tim*, *vri*, and *Pdp1* are the only overlap between the 24 clock-driven genes in larval LN_vs and the ~100 genes with circadian expression identified by a meta-analysis of multiple whole head microarray studies (Wijnen et al., 2006). While this supports the idea that novel information comes from using a single cell type for expression profiling, added power will come from additional time points and replicates. Nevertheless, the spatial-resolution in the LN_v dataset

and resulting small list of clock-driven LN_v genes will permit detailed studies of their contribution to LN_v function.

Circadian gene expression profiles

To validate the GeneChip data, we focused on genes whose expression is clock-driven and enriched. These are the four core clock genes (*per*, *tim*, *vri* and *Pdp1*) and six genes previously unstudied in LN_vs: *Ir*, which encodes an Inwardly rectifying K^+ channel; *CG33275*, predicted to encode a Rho-GEF; *Pka-C3* and three uncharacterized genes (*CG14521*, *CG42238* and *CG14853*).

Figures 2A and 2B show the expression profiles for 9 of the genes that are both clock-driven and enriched as well as for *Pdf*, a non-cycling enriched gene. Rhythmic expression in LD and clock-regulation made it likely that all of these genes would also be rhythmically expressed in constant darkness (DD), the hallmark of circadian gene regulation. This has already been demonstrated in larval and/or adult LN_vs for *tim*, *vri*, *Pdp1* and *cry* RNA (Price et al., 1998; Yang and Sehgal, 2001; Peng et al., 2003; JB, unpublished data). To validate rhythmic LN_v expression for the previously unstudied genes and to test for rhythms in DD, LN_vs were isolated from wild-type larvae at four timepoints on the second day in DD after prior entrainment to LD cycles. RNA was isolated from FACS-sorted LN_vs as for the GeneChip experiments. mRNA was then amplified using a method that includes random priming and expression levels were measured by qPCR. Thus the amplification and quantification strategies differ from the GeneChip studies, which used a poly-T driven amplification.

Figure 2C shows the results of qPCR using primers to amplify *cry*, *Ir*, *per* and *Pdp1* from RNA isolated at four different time points in DD. The results show circadian rhythms in gene expression for all four genes. We detected peak levels of *cry* at CT10 and trough levels at CT16, whereas *Ir*, *per* and *Pdp1* RNAs have a different phase with peak levels at CT10/CT16 and trough levels at CT4 and CT22. The results in Figure 2D also show robust oscillations in DD for all 5 genes: *Pka-C3, CG14853 and CG14521* are all at much higher levels at CT10 than CT22 (as seen for *cry*); *CG33275* seems to oscillate in phase with *per*, *Ir* and *Pdp1*, with high levels at CT16 and trough levels at CT4. *CG42238* RNA levels are highest at CT22. These qPCR data extend the conclusions from the GeneChip experiments since strong circadian rhythms in gene expression were detected for all 6 novel LN_v genes.

Altered expression of *Ir* in LN_vs affects circadian behavior

Clock-driven oscillations in *Ir* expression could be one mechanism by which LN_vs generate circadian rhythms in excitability since Inward rectifier K^+ channels regulate resting membrane potential in mammals (Hille, 2001; Kuhlman and McMahon, 2006). More Inward rectifiers at the cell membrane should increase K^+ efflux, hyperpolarizing the cell, while decreased Ir levels should decrease K^+ efflux and depolarize the cell. The temporal profile of *Ir* expression (Figure 2C) is consistent with electrophysiological measurements of adult s-LN_vs, which become progressively depolarized towards the end of the night when *Ir* expression is low, and then start to hyperpolarize again after dawn when *Ir* RNA levels begins to rise (Cao and Nitabach, 2008).

We first tested a role for *Ir* in LN_v function using larval light avoidance. In this assay, larvae are placed in the middle of a Petri dish half of which is exposed to light and the number of larvae on the dark side is counted 15 minutes later. Wild type larvae show a robust preference for the dark side, with ~70% in the dark after 15min at bright light. LN_vs are downstream of the larval visual system and their neuronal activity rapidly increases with light exposure. This response is elevated when LN_vs are made hyper-excitable by expressing *NaChBac*, a low threshold voltage-gated sodium channel (Yuan et al., 2011). This likely explains how larvae with *Pdf-Gal4* expressing *NaChBac* in LN_vs avoid low light levels much better than control larvae (Collins et al., 2012; Figure 3A).

We tested the effect of knocking-down *Ir* expression specifically in LN_vs using *Pdf-Gal4* to express a UAS transgene that expresses RNAi directed to *Ir* (*UAS-Ir:RNAi*) at ZT15, when *Ir* expression is high. The results in Figure 3A show that knocking-down *Ir* in LN_vs made larvae super-sensitive to low light (30lux), compared to control *UAS-Ir:RNAi* or *Pdf-Gal4* larvae. The similar light avoidance phenotypes of larvae in which LN_vs either express NaChBac or *Ir:RNAi* are consistent with the idea that *Ir* levels in LN_vs are inversely related to LN_v excitability.

To quantify the efficacy of *Ir:RNAi*, LN_vs were isolated by FACS from either control larvae (*UAS-Ir:RNAi* alone) or with *Pdf-Gal4* expressing *UAS-Ir:RNAi* at ZT15. mRNA was amplified and gene expression measured by qPCR. The results in Figure 3B show a 3.8-fold decrease in *Ir* transcript abundance in larval LN_vs expressing *Pdf-Gal4* and *UAS-Ir:RNAi*, verifying that the *UAS-Ir:RNAi* transgene reduces *Ir* RNA levels in LN_vs.

Altered *Ir* expression in adult LN_vs changes circadian locomotor activity

One reason for profiling larval LN_vs was to identify key genes expressed in adult s-LN_vs without the confounding issue of co-purifying l-LN_vs. To test a role for *Ir* in adult LN_vs, we measured the locomotor activity rhythms of flies with *Pdf-Gal4* expressing *UAS-Ir:RNAi*. These flies had strong 25.0hr long period locomotor rhythms in DD compared to control flies with periods between 23.6 and 24.5hr (Figure 3C, Table S4). Long-period behavioral rhythms are also seen when LN_vs are hyper-excited via *UAS-NaChBac*, which leads to a dominant 25.5hr behavioral period as well as complex behavioral rhythms (Nitabach et al., 2006), or via *UAS-dnATPase* [a dominant-negative Na^+/K^+-ATPase α subunit (Sun et al., 2001), Table S4]. The similar period phenotypes of flies with *Pdf-Gal4* expressing *UAS-Ir:RNAi*, *UAS-NaChBac* or *UAS-dnATPase* are consistent with decreased *Ir* expression increasing LN_v excitability and further support the idea that *Ir* expression levels regulate LN_v excitability.

A similar long period rhythm was observed when *Ir-RNAi* expression was widened to include all adult clock neuron groups using the *tim(UAS)-Gal4* driver (Figure 3C, Table S4). This was surprising because *tim(UAS)-Gal4* usually gives stronger phenotypes than *Pdf-Gal4* and because hyper-exciting all clock neurons with *tim(UAS)-Gal4* and *UAS-NaChBac* makes flies arrhythmic (Collins et al., 2012). This suggested that *Ir* might not play a role in other clock neurons. To test this idea, *UAS-Ir:RNAi* was expressed in all clock neurons except LN_vs, using the *tim(UAS)-Gal4* driver in combination with a *Pdf-Gal80* transgene that inhibits Gal4 activity specifically in LN_vs (Stoleru et al., 2004). The results in Figure 3C

and Table S4 show that flies in which *Ir:RNAi* was restricted to non-LN_v clock neurons have normal circadian rhythms. This contrasts with expressing NaChBac only in non-LN_v clock neurons, which dramatically constricts the time when flies are active (Collins et al., 2012). Thus *Ir* does not seem to regulate non-LN_v clock neurons and is perhaps not even expressed in non-LN_v clock neurons.

To test where *Ir* is expressed, we used a Gal4 enhancer trap inserted in *Ir* (NP2554, hereafter referred to as Ir^{Gal4}). *Ir-Gal4* flies were crossed to a *UAS-nuclear-YFP* transgene (Kimura, 2005). Brains were dissected at ZT15 and stained for YFP, PDF (to mark LN_vs) and VRI (to mark all clock neurons). Nuclear YFP was detected in all four adult PDF+ s-LN_vs (Figure 3D) in all 10 brains examined. We found YFP expressed in 2–3 of the 5 l-LN_vs but not in the 5th PDF- s-LN_v. We found YFP expressed in one of the six LN_ds (Dorsal lateral neurons), but in none of the three dorsal neuron (DN) groups, although it is difficult to completely exclude expression in DNs since they are numerous and reside in different focal planes. The relatively broad expression of *Ir-Gal4* in the brain is consistent with *Ir* being one of only 3 Inward Rectifier K^+ channels in the *Drosophila* genome and underlines the importance of purifying LN_vs prior to expression profiling to detect rhythmic *Ir* expression. Although this Ir^{Gal4} enhancer trap line might not precisely reflect *Ir* expression, the pattern seen is consistent with the genetic data above indicating that s-LN_vs are the main locus where *Ir* acts in circadian rhythms. This interpretation is consistent with Nagoshi et al., (2010) who detected high-level *Ir* expression in larval and adult LN_vs but not in other clock neurons. In addition, Kula-Eversole et al., (2010) found that *Ir* is rhythmically expressed in adult LN_vs.

Increased *Ir* expression disrupts behavioral rhythms and the LN_v molecular clock

As an additional test of the importance of *Ir* in circadian rhythms, we assayed a novel *Ir* P-element insertion line (Ir^{d08240}, referred to hereafter as Ir^d). We found that 47% of Ir^d flies were arrhythmic. This phenotype was reverted by excising the P-element ($Ir^{d\ rev}$, Fig. 4A). To understand how Ir^d affected *Ir* expression, we measured *Ir* levels in RNA extracted from whole fly heads. The results in Fig. 4B show a modest but significant increase in *Ir* RNA in Ir^d flies compared to control (1.6–1.8-fold). $Ir^{d\ rev}$ flies had the same *Ir* expression levels as control flies, indicating that *Ir* over-expression likely underlies the behavioral defects. However, we have not determined how strongly *Ir* is over-expressed in Ir^d LN_vs. Heterozygous Ir^d flies also have a higher incidence of arrhythmicity than control flies, consistent with increased *Ir* expression via this gain-of-function mutation (DM & JB, data not shown).

Since the Ir^d mutation does not target LN_vs specifically, we measured molecular clock oscillations in LN_vs to test if these are affected by increased *Ir* expression. Over-expressing *Ir* in LN_vs should hyper-polarize these cells. Interestingly, the behavioral phenotype of Ir^d mutants is similar to LN_vs expressing the dORKΔ K^+ channel (Nitabach et al., 2002), which causes LN_v molecular clocks to run-down with the constitutively-expressed *Pdf-Gal4* driver (Nitabach et al., 2002; Nitabach et al., 2005). A mammalian inward rectifier K+ channel (mKir2.1) expressed in LN_vs also hyperpolarized LN_vs and caused their molecular clocks to run down (Nitabach et al., 2002; Nitabach et al., 2005; Wu et al., 2008), leading to the idea

that the LN_v molecular clock requires LN_v membrane activity for robust rhythms in DD. However, this idea was challenged when Depetris-Chauvin et al., (2011) found that expressing mKir2.1 only in adulthood via an inducible *Pdf-Gal4* made flies arrhythmic but did not dramatically affect their molecular clocks. However, it has not yet been tested how strongly the constitutive and inducible mKir2.1 expression affect LN_v resting membrane potential. The long periods seen with *Ir:RNAi* (Fig. 3C) suggest that *Ir*, as an endogenous ion channel, likely affects molecular clock oscillations and contributes to period determination. To test how *Ir* over-expression affects the LN_v molecular clock, we measured PER protein rhythms in the s-LN_vs of Ir^d and $Ir^{d\ rev}$ adult flies on day 5 in DD. The results in Figure 4C–D show that peak PER protein levels at CT23 are reduced in Ir^d flies (t-test, $p<0.05$). Taking these data together with the modest period-lengthening in *Ir:RNAi* flies leads us to propose that *Ir* is not just a clock output, but likely affects LN_v excitability which, in turn, feeds back to regulate the molecular clock by, as yet, unidentified mechanisms.

Discussion

Expression profiling of *Drosophila* pacemaker neurons

Circadian rhythms offer one of the best examples of how genes regulate animal behavior. However, there have been relatively few insights into how molecular clocks control pacemaker neuronal activity rhythms. Since circadian rhythms in mRNA levels are widespread across organisms (e.g. Harmer et al., 2000; Storch et al., 2002; Wijnen et al., 2006), rhythmic expression of key output genes that underlie rhythmic pacemaker neuron activity is an attractive idea. Our approach to identifying clock-regulated output genes differed from most previous circadian expression profiling studies by starting with a homogeneous population of behaviorally-relevant pacemaker neurons. Single-cell type expression profiling is clearly a powerful approach because the vast majority of rhythmically expressed transcripts identified in larval LN_vs (this study) or adult l-LN_vs (Kula-Eversole et al., 2010) differ from those showing rhythmic expression in whole fly heads.

Ir contributes to the regulation of LN_v excitability

We focused on *Ir* because of the well-described roles of Inward Rectifier K^+ channels in resting membrane potential and neuronal activity (Hille, 2001). Since *Ir* transcript levels are high at CT10 and CT16 (around dusk) and low at CT22 and CT4 (around dawn), LN_vs should be less excitable at dusk than at dawn. This inference correlates well with electrophysiological measurements of adult s-LN_v resting membrane potential, which becomes progressively depolarized towards the end of the night (Cao and Nitabach, 2008). Low *Ir* expression in cyc^0 mutants and high expression in per^0 mutants is consistent with data indicating that larval LN_v excitability is high when CLK/CYC activity is low (Collins et al., 2012). Ultimately these ideas will require measuring when Ir protein is present and functional. We note that the ~365aa cytoplasmic C-terminus of Ir has 63 Serines and Threonines, suggesting that phosphorylation may also regulate Ir activity. Low *Ir* RNA levels in LN_vs at dawn, and thus high LN_v excitability, are consistent with LN_vs promoting: (i) larval light avoidance, which peaks around dawn (Mazzoni et al., 2005), and (ii) the

morning peak of adult locomotor activity in LD cycles (Grima et al., 2004; Stoleru et al., 2004). The presence of multiple E boxes (potential CLK/CYC binding sites) in the *Ir* regulatory region (MR & JB, data not shown), its phase of expression and the effect of the per^0 and cyc^0 mutations on *Ir* RNA levels support the idea that *Ir* is a direct CLK/CYC target, although this remains to be formally tested.

Although *Ir* is rhythmically expressed in LN_vs, we propose that other clock neurons have different mechanism(s) to link their molecular clocks to neuronal activity. Larval LN_vs and DN1s have opposite relationships between CLK/CYC activity and excitability: LN_vs are most excitable when CLK/CYC activity is low and DN1s are most excitable when CLK/CYC activity is high (Collins et al., 2012). Cell-type specific clock outputs have already been observed in mammals, where similarly phased molecular clocks lead to rhythmic expression of outputs that differ extensively between tissues (e.g. Storch et al., 2002). Similarly, we propose that CLK/CYC regulate distinct sets of output genes in different clock neurons.

A holistic model for regulating LN_v output

While *Ir* affects circadian behavior, the rhythmic physiology of LN_vs probably derives from multiple genes and/or redundant mechanisms, perhaps explaining why forward genetics has revealed little about clock outputs. Our LN_v GeneChips identify additional clock-driven genes with potential roles in clock output, including *amon*, an enzyme that cleaves inactive neuropeptide precursors, *Snap* (*Soluble NSF attachment protein*), which helps recycle synaptic vesicles from the plasma membrane and *Rdl*, a GABA-activated chloride channel.

It will be interesting to determine how similar the mechanisms for regulating circadian rhythms in excitability are between *Drosophila* and mammals. For the SCN, rhythms in excitability can be sub-divided into rhythms in resting membrane potential and action potential frequency (Kuhlman and McMahon, 2006). No channels have yet been identified that regulate SCN membrane potential, but firing frequency is likely regulated by BK, Kv3.1 and Kv3.2 K^+ channels (Itri et al., 2005; Meredith et al., 2006; Kudo et al., 2011). Although mice lacking either BK or both Kv3.1 and Kv3.2 display weakened behavioral rhythms, no altered periods were seen (Meredith et al., 2006; Kudo et al., 2011). However, manipulating the channel(s) that determine resting membrane potential in SCN neurons may change period length because artificially hyper-polarizing SCN slices *in vitro* with low K^+ altered period and/or lead to loss of *mPer1*-luciferase rhythms (Lundkvist et al., 2005), suggesting a link between membrane potential and the molecular clock. At least for *Drosophila*, the period-altering phenotypes with *Ir* knockdown and LN_v hyper-excitation (e.g. via NaChBac) blur the conventional distinction between clock outputs and inputs.

In conclusion, whole-genome profiling of purified LN_vs presents an exceptional opportunity to link the transcriptional profile of a single neuronal type to animal behavior. Our results also suggest multiple levels of regulating LN_v activity and give us a short list of genes for targeted manipulation in LN_vs. Generating transcriptional profiles of individual neuronal types should be broadly applicable in neurobiology to analyze how defined neuronal populations use regulated transcription to shape, for example, sex-specific behavioral traits

(Ryner et al., 1996) and other complex cognitive processes (Klausberger and Somogyi, 2008).

Supplementary Material

Refer to Web version on PubMed Central for supplementary material.

Acknowledgments

We gratefully acknowledge Jason Rihel for suggesting this approach to clock neuron function, Paul D'Agostino and Esteban Mazzoni for encouraging us to use FACS, Chris Wegener for the cell dissociation protocol, Ben Collins and Dave Reeves for creating *Pdf-RFP* flies and Alex Keene for designing the larval light box. Special thanks to Ben Collins and David Dahdal for early morning dissections and to John Hirst, Peter Lopez and Gelo Victoriano de la Cruz for FACS. We also thank Ken Birnbaum, Mark Siegal and John Hogenesch for advice on FACS and GeneChip analysis and Ryan Baugh for advice on RNA amplification. We thank Jeff Hall, Paul Hardin, Mike Nitabach, Michael Rosbash, Paul Salvaterra, Simon Sprecher, Roger Tsien, the Developmental Studies Hybridoma Bank, the *Drosophila* Genetic Resource Center (Japan), the National Institute of Genetics (Japan) and the Vienna *Drosophila* RNAi Center for flies, antibodies and DNA. We thank Emi Nagoshi and Michael Rosbash for sharing data prior to publication, Frank Doring and Claude Desplan for many invaluable discussions on all aspects of this project and Matthieu Cavey, Ben Collins and David Dahdal for comments on the manuscript. This investigation was conducted in a facility constructed with support from Research Facilities Improvement Grant Number C06 RR-15518-01 from the NCRR, NIH and in the NYU Center for Genomics & Systems Biology Core Facility. The NYUCI flow cytometry core is supported by NIH/NCI grant P30CA16087-31. This work was supported by an NYU Dean's Dissertation fellowship (DM) and NIH grants NRSA F32 GM72197 (MDD) and GM063911 (JB).

References

Belle MD, Diekman CO, Forger DB, Piggins HD. Daily electrical silencing in the mammalian circadian clock. Science. 2009; 326:281–284. [PubMed: 19815775]

Blalock EM, Chen KC, Sharrow K, Herman JP, Porter NM, Foster TC, Landfield PW. Gene microarrays in hippocampal aging: statistical profiling identifies novel processes correlated with cognitive impairment. J Neurosci. 2003; 23:3807–3819. [PubMed: 12736351]

Blanchard FJ, Collins B, Cyran SA, Hancock DH, Taylor MV, Blau J. The transcription factor Mef2 is required for normal circadian behavior in *Drosophila*. J Neuroscience. 2010; 30:5855–5865.

Calza S, Raffelsberger W, Ploner A, Sahel J, Leveillard T, Pawitan Y. Filtering genes to improve sensitivity in oligonucleotide microarray data analysis. Nucleic Acids Res. 2007; 35:e102. [PubMed: 17702762]

Cao G, Nitabach MN. Circadian control of membrane excitability in *Drosophila melanogaster* lateral ventral clock neurons. J Neurosci. 2008; 28:6493–6501. [PubMed: 18562620]

Chung BY, Kilman VL, Keath JR, Pitman JL, Allada R. The $GABA_A$ receptor RDL acts in peptidergic PDF neurons to promote sleep in *Drosophila*. Curr Biol. 2009; 19:386–390. [PubMed: 19230663]

Collins B, Kane EA, Reeves DC, Akabas MH, Blau J. Balance of activity between LNvs and glutamatergic dorsal clock neurons promotes robust circadian rhythms in *Drosophila*. Neuron. 2012; 74:706–718. [PubMed: 22632728]

Cyran SA, Yiannoulos G, Buchsbaum AM, Saez L, Young MW, Blau J. The Double-Time protein kinase regulates the subcellular localization of the *Drosophila* clock protein Period. J Neurosci. 2005; 25:5430–5437. [PubMed: 15930393]

Depetris-Chauvin A, Berni J, Aranovich EJ, Muraro NI, Beckwith EJ, Ceriani MF. Adult-specific electrical silencing of pacemaker neurons uncouples molecular clock from circadian outputs. Curr Biol. 2011; 21:1783–1793. [PubMed: 22018542]

Grima B, Chelot E, Xia R, Rouyer F. Morning and evening peaks of activity rely on different clock neurons of the *Drosophila* brain. Nature. 2004; 431:869–873. [PubMed: 15483616]

Hardin PE. Molecular genetic analysis of circadian timekeeping in *Drosophila*. Advances in genetics. 2011; 74:141–173. [PubMed: 21924977]

Harmer SL, Hogenesch JB, Straume M, Chang HS, Han B, Zhu T, Wang X, Kreps JA, Kay SA. Orchestrated transcription of key pathways in *Arabidopsis* by the circadian clock. Science. 2000; 290:2110–2113. [PubMed: 11118138]

Herzog ED, Takahashi JS, Block GD. *Clock* controls circadian period in isolated suprachiasmatic nucleus neurons. Nat Neurosci. 1998; 1:708–713. [PubMed: 10196587]

Hille, B. Ion channels of excitable membranes. 3. Sinauer Associates; 2001.

Irizarry RA, Bolstad BM, Collin F, Cope LM, Hobbs B, Speed TP. Summaries of Affymetrix GeneChip probe level data. Nucleic Acids Res. 2003; 31:e15. [PubMed: 12582260]

Itri JN, Michel S, Vansteensel MJ, Meijer JH, Colwell CS. Fast delayed rectifier potassium current is required for circadian neural activity. Nat Neurosci. 2005; 8:650–656. [PubMed: 15852012]

Jagota A, de la Iglesia HO, Schwartz WJ. Morning and evening circadian oscillations in the suprachiasmatic nucleus in vitro. Nat Neurosci. 2000; 3:372–376. [PubMed: 10725927]

Keegan KP, Pradhan S, Wang JP, Allada R. Meta-analysis of *Drosophila* circadian microarray studies identifies a novel set of rhythmically expressed genes. PLoS Comput Biol. 2007; 3:e208. [PubMed: 17983263]

Kimura H. Histone dynamics in living cells revealed by photobleaching. DNA repair. 2005; 4:939–950. [PubMed: 15905138]

Klausberger T, Somogyi P. Neuronal diversity and temporal dynamics: the unity of hippocampal circuit operations. Science. 2008; 321:53–57. [PubMed: 18599766]

Kudo T, Loh DH, Kuljis D, Constance C, Colwell CS. Fast delayed rectifier potassium current: critical for input and output of the circadian system. J Neurosci. 2011; 31:2746–2755. [PubMed: 21414897]

Kuhlman SJ, McMahon DG. Encoding the ins and outs of circadian pacemaking. J Biol Rhythms. 2006; 21:470–481. [PubMed: 17107937]

Kula-Eversole E, Nagoshi E, Shang Y, Rodriguez J, Allada R, Rosbash M. Surprising gene expression patterns within and between PDF-containing circadian neurons in *Drosophila*. Proc Natl Acad Sci U S A. 2010; 107:13497–13502. [PubMed: 20624977]

Liu C, Weaver DR, Strogatz SH, Reppert SM. Cellular construction of a circadian clock: period determination in the suprachiasmatic nuclei. Cell. 1997; 91:855–860. [PubMed: 9413994]

Lundkvist GB, Kwak Y, Davis EK, Tei H, Block GD. A calcium flux is required for circadian rhythm generation in mammalian pacemaker neurons. J Neurosci. 2005; 25:7682–7686. [PubMed: 16107654]

Mazzoni EO, Desplan C, Blau J. Circadian pacemaker neurons transmit and modulate visual information to control a rapid behavioral response. Neuron. 2005; 45:293–300. [PubMed: 15664180]

Meredith AL, Wiler SW, Miller BH, Takahashi JS, Fodor AA, Ruby NF, Aldrich RW. BK calcium-activated potassium channels regulate circadian behavioral rhythms and pacemaker output. Nat Neurosci. 2006; 9:1041–1049. [PubMed: 16845385]

Michel S, Geusz ME, Zaritsky JJ, Block GD. Circadian rhythm in membrane conductance expressed in isolated neurons. Science. 1993; 259:239–241. [PubMed: 8421785]

Nagoshi E, Sugino K, Kula E, Okazaki E, Tachibana T, Nelson S, Rosbash M. Dissecting differential gene expression within the circadian neuronal circuit of *Drosophila*. Nat Neurosci. 2010; 13:60–68. [PubMed: 19966839]

Nitabach MN, Blau J, Holmes TC. Electrical silencing of *Drosophila* pacemaker neurons stops the free-running circadian clock. Cell. 2002; 109:485–495. [PubMed: 12086605]

Nitabach MN, Sheeba V, Vera D, Blau J, Holmes TC. Membrane electrical excitability is necessary for the free-running larval *Drosophila* circadian clock. J Neurobiol. 2005; 62:1–13. [PubMed: 15389695]

Nitabach MN, Wu Y, Sheeba V, Lemon WC, Strumbos J, Zelensky PK, White BH, Holmes TC. Electrical hyperexcitation of lateral ventral pacemaker neurons desynchronizes downstream circadian oscillators in the fly circadian circuit and induces multiple behavioral periods. J Neurosci. 2006; 26:479–489. [PubMed: 16407545]

Panda S, Antoch MP, Miller BH, Su AI, Schook AB, Straume M, Schultz PG, Kay SA, Takahashi JS, Hogenesch JB. Coordinated transcription of key pathways in the mouse by the circadian clock. Cell. 2002; 109:307–320. [PubMed: 12015981]

Parisky KM, Agosto J, Pulver SR, Shang Y, Kuklin E, Hodge JJ, Kang K, Liu X, Garrity PA, Rosbash M, et al. PDF cells are a GABA-responsive wake-promoting component of the *Drosophila* sleep circuit. Neuron. 2008; 60:672–682. [PubMed: 19038223]

Park JH, Helfrich-Forster C, Lee G, Liu L, Rosbash M, Hall JC. Differential regulation of circadian pacemaker output by separate clock genes in *Drosophila*. Proc Natl Acad Sci U S A. 2000; 97:3608–3613. [PubMed: 10725392]

Peng Y, Stoleru D, Levine JD, Hall JC, Rosbash M. *Drosophila* free-running rhythms require intercellular communication. PLoS Biol. 2003; 1:32–40.

Price JL, Blau J, Rothenfluh A, Abodeely M, Kloss B, Young MW. *double-time* is a novel *Drosophila* clock gene that regulates PERIOD protein accumulation. Cell. 1998; 94:83–95. [PubMed: 9674430]

Ryner LC, Goodwin SF, Castrillon DH, Anand A, Villella A, Baker BS, Hall JC, Taylor BJ, Wasserman SA. Control of male sexual behavior and sexual orientation in *Drosophila* by the *fruitless* gene. Cell. 1996; 87:1079–1089. [PubMed: 8978612]

Saeb-Parsy K, Dyball RE. Defined cell groups in the rat suprachiasmatic nucleus have different day/night rhythms of single-unit activity in vivo. J Biol Rhythms. 2003; 18:26–42. [PubMed: 12568242]

Shaner NC, Campbell RE, Steinbach PA, Giepmans BN, Palmer AE, Tsien RY. Improved monomeric red, orange and yellow fluorescent proteins derived from *Discosoma* sp. red fluorescent protein. Nature biotechnology. 2004; 22:1567–1572.

Shang Y, Griffith LC, Rosbash M. Light-arousal and circadian photoreception circuits intersect at the large PDF cells of the *Drosophila* brain. Proc Natl Acad Sci U S A. 2008; 105:19587–19594. [PubMed: 19060186]

Sheeba V, Fogle KJ, Kaneko M, Rashid S, Chou YT, Sharma VK, Holmes TC. Large ventral lateral neurons modulate arousal and sleep in *Drosophila*. Curr Biol. 2008; 18:1537–1545. [PubMed: 18771923]

Stoleru D, Peng Y, Agosto J, Rosbash M. Coupled oscillators control morning and evening locomotor behaviour of *Drosophila*. Nature. 2004; 431:862–868. [PubMed: 15483615]

Stoleru D, Peng Y, Nawathean P, Rosbash M. A resetting signal between *Drosophila* pacemakers synchronizes morning and evening activity. Nature. 2005; 438:238–242. [PubMed: 16281038]

Storch KF, Lipan O, Leykin I, Viswanathan N, Davis FC, Wong WH, Weitz CJ. Extensive and divergent circadian gene expression in liver and heart. Nature. 2002; 417:78–83. [PubMed: 11967526]

Storey JD, Tibshirani R. Statistical significance for genomewide studies. Proc Natl Acad Sci U S A. 2003; 100:9440–9445. [PubMed: 12883005]

Sun B, Xu P, Wang W, Salvaterra PM. In vivo modification of Na^+/K^+-ATPase activity in *Drosophila*. Comp Biochem & Phys Part B, Biochemistry & molecular biology. 2001; 130:521–536.

Wegener C, Hamasaka Y, Nassel DR. Acetylcholine increases intracellular Ca^{2+} via nicotinic receptors in cultured PDF-containing clock neurons of *Drosophila*. J Neurophysiol. 2004; 91:912–923. [PubMed: 14534288]

Welsh DK, Logothetis DE, Meister M, Reppert SM. Individual neurons dissociated from rat suprachiasmatic nucleus express independently phased circadian firing rhythms. Neuron. 1995; 14:697–706. [PubMed: 7718233]

Wijnen H, Naef F, Boothroyd C, Claridge Chang A, Young MW. Control of daily transcript oscillations in *Drosophila* by light and the circadian clock. PLoS Genet. 2006; 2:e39. [PubMed: 16565745]

Wu Y, Cao G, Nitabach MN. Electrical silencing of PDF neurons advances the phase of non-PDF clock neurons in *Drosophila*. J Biol Rhythms. 2008; 23:117–128. [PubMed: 18375861]

Yang Z, Sehgal A. Role of molecular oscillations in generating behavioral rhythms in *Drosophila*. Neuron. 2001; 29:453–467. [PubMed: 11239435]

Yuan Q, Xiang Y, Yan Z, Han C, Jan LY, Jan YN. Light-induced structural and functional plasticity in *Drosophila* larval visual system. Science. 2011; 333:1458–1462. [PubMed: 21903815]

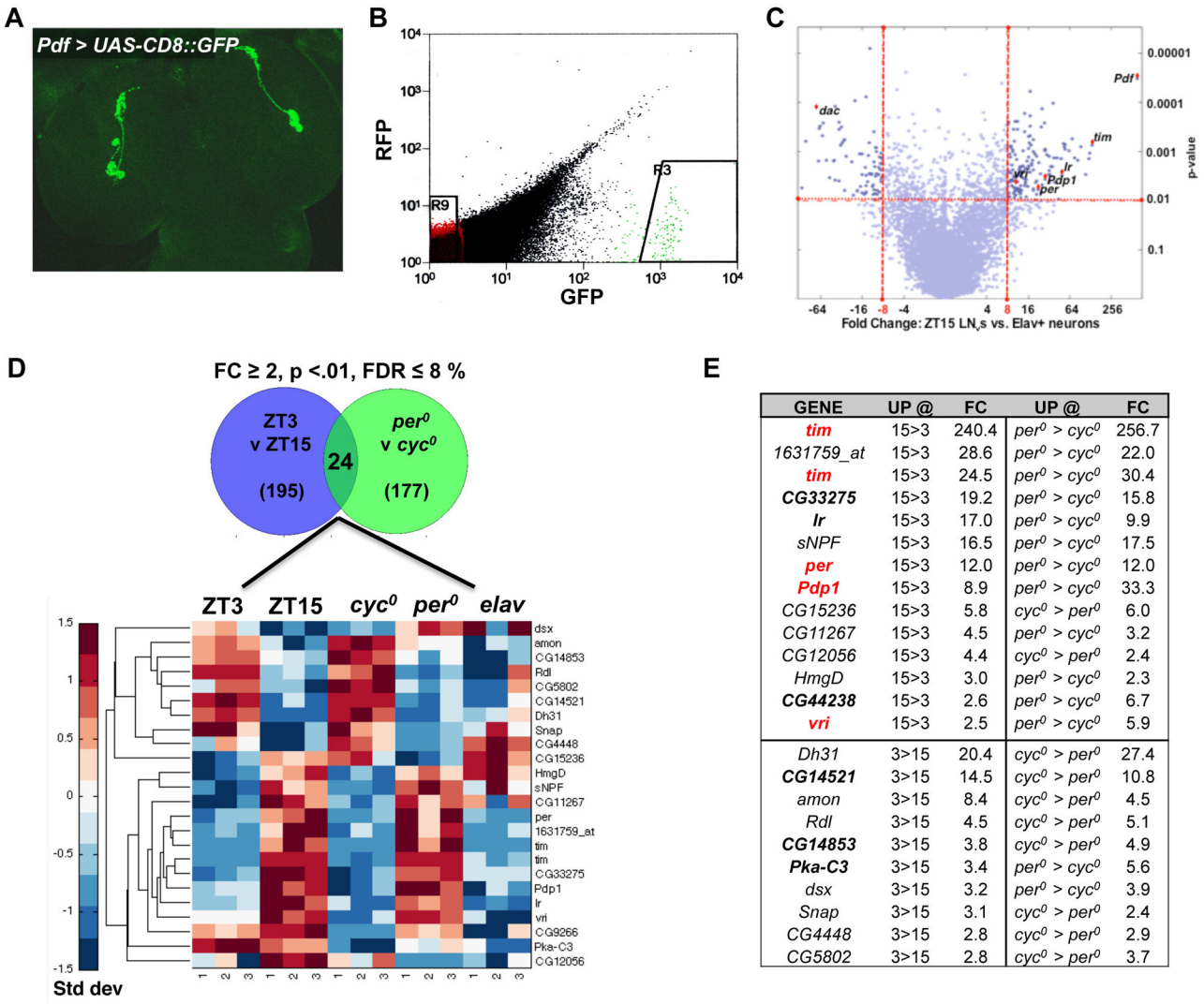

GENE	UP @	FC	UP @	FC
tim	15>3	240.4	per^0 > cyc^0	256.7
1631759_at	15>3	28.6	per^0 > cyc^0	22.0
tim	15>3	24.5	per^0 > cyc^0	30.4
CG33275	15>3	19.2	per^0 > cyc^0	15.8
Ir	15>3	17.0	per^0 > cyc^0	9.9
sNPF	15>3	16.5	per^0 > cyc^0	17.5
per	15>3	12.0	per^0 > cyc^0	12.0
Pdp1	15>3	8.9	per^0 > cyc^0	33.3
CG15236	15>3	5.8	cyc^0 > per^0	6.0
CG11267	15>3	4.5	per^0 > cyc^0	3.2
CG12056	15>3	4.4	cyc^0 > per^0	2.4
HmgD	15>3	3.0	per^0 > cyc^0	2.3
CG44238	15>3	2.6	per^0 > cyc^0	6.7
vri	15>3	2.5	per^0 > cyc^0	5.9
Dh31	3>15	20.4	cyc^0 > per^0	27.4
CG14521	3>15	14.5	cyc^0 > per^0	10.8
amon	3>15	8.4	cyc^0 > per^0	4.5
Rdl	3>15	4.5	cyc^0 > per^0	5.1
CG14853	3>15	3.8	cyc^0 > per^0	4.9
Pka-C3	3>15	3.4	per^0 > cyc^0	5.6
dsx	3>15	3.2	per^0 > cyc^0	3.9
Snap	3>15	3.1	cyc^0 > per^0	2.4
CG4448	3>15	2.8	cyc^0 > per^0	2.9
CG5802	3>15	2.8	cyc^0 > per^0	3.7

Figure 1. Identification of genes enriched in larval pacemaker neurons that are also time- and clock-dependent

(A) Whole-mount of larval brain lobes with *Pdf-Gal4* expressing *UAS-CD8:GFP*. GFP antibodies label four LN_vs in each lobe.

(B) FACS scatter plot shows the .01% most-GFP+ cells (gate R3). Collected GFP^+ cells are roughly 2–3 orders of magnitude more fluorescent than GFP− cells of the same size (gate R9). GFP^+ cells group together by size (data not shown).

(C) Gene expression in larval LN_vs isolated at ZT15 vs. Elav+ neurons. Each blue circle represents one of the 18,952 GeneChip probes covering the *Drosophila* genome. Fold change in LN_vs vs. Elav+ neurons is plotted on the x-axis and p-value (t-test) on the y-axis. Cutoff lines at 8-fold and .01 p-value show mRNAs with significantly enriched expression in LN_vs compared to Elav+ cells at ZT15. Core clock genes and *Ir* are highlighted with red diamonds, as is the de-enriched gene *dac (dachsund)*.

(D) 24 mRNAs (23 unique genes) are rhythmically expressed and clock-regulated (clock-driven, p-value < 0.01, FDR < 8% and fold change > 2) when comparing LN_vs at ZT3 vs. ZT15 (195 mRNAs) and per^0 vs. cyc^0 (177 mRNAs). Plots below the pie charts show

expression values for these 24 mRNAs (rows) across five genomic conditions with three replicates for each (columns). Values were standardized by mean centering (row mean = 0, row standard deviation =1) and assigned color-map values based on their standard deviation from the row mean. Rows were clustered using the Euclidean pairwise distance algorithm. (E) Fold changes (FC) for clock-driven mRNAs. The charts show the clock-driven transcripts whose expression is higher at ZT15 than ZT3 (top) or higher at ZT3 than ZT15 (bottom). FC = fold change of the mean of 3 replicates each for ZT 3, ZT 15, per^{0} and cyc^{0}. See Methods for statistical analyses. The "UP @" columns shows whether expression of that transcript was higher at ZT15 or ZT3 (left column) or in per^{0} or cyc^{0} LN_vs. (right). Expression of 10 of these 23 clock-driven genes was also significantly enriched in LN_vs compared to Elav+ neurons (indicated in bold). 4 of these 10 genes are core clock genes (indicated in red).

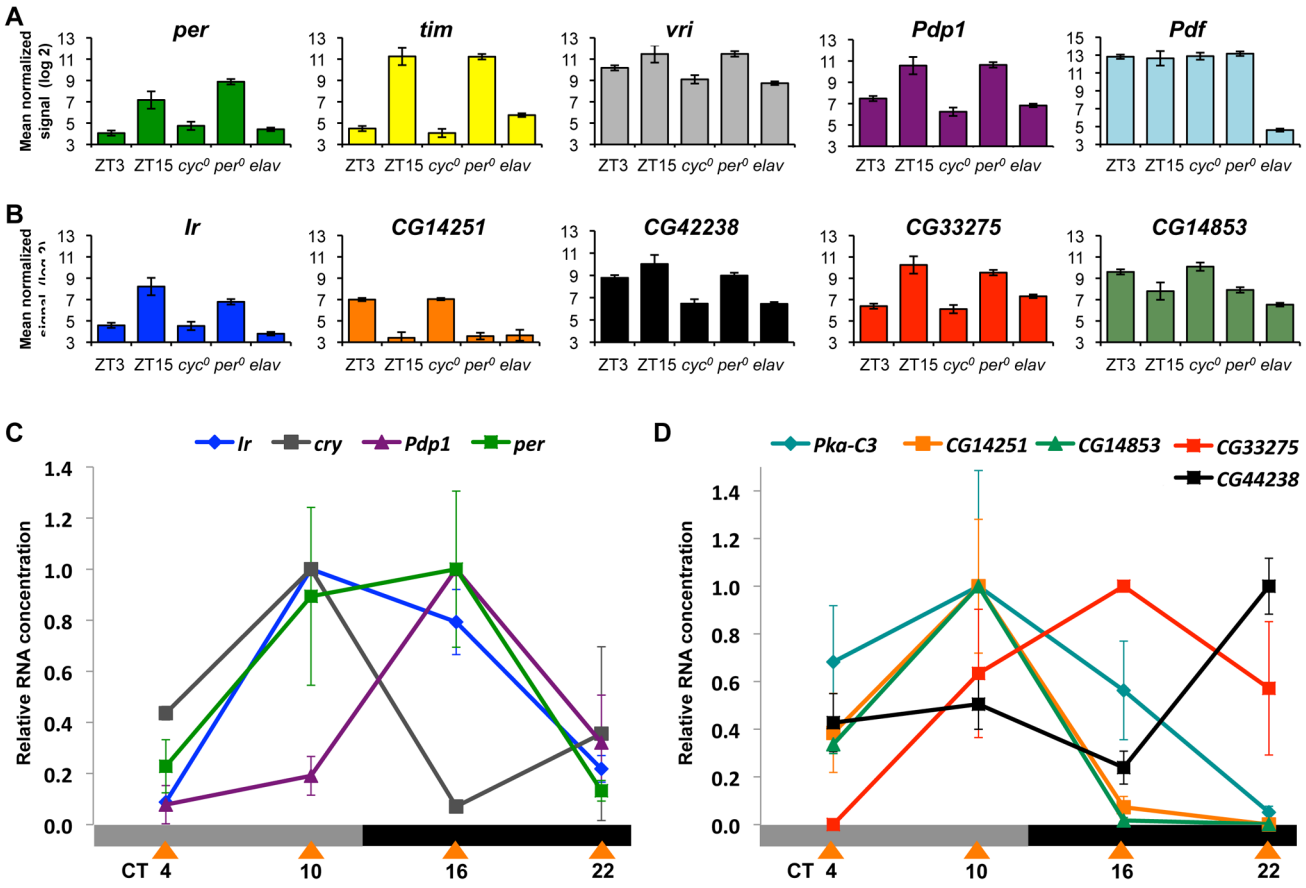

Figure 2. Clock-driven transcript profiles across time, genotype, and cell type

(A) Hybridization signal (y-axis) for the CLK/CYC direct target genes *per*, *tim*, *vri* and *Pdp1*. The signal represents the mean normalized and log-transformed hybridization intensity for the 3 replicate experiments at each timepoint. Error bars indicate standard error of the mean (SEM). The hybridization signal to *Pdf* is also shown.

(B) Signals for five additional enriched and clock-driven genes in LN_vs.

(C) Real-time qPCR on amplified LN_v RNA for *Ir* (blue diamonds), *Pdp1* (purple triangles), *cry* (grey squares) and *per* (green squares) at four time points on day 2 of constant darkness (circadian time, CT). For all qPCR experiments, RNA levels were normalized to non-cycling levels of *Pdf*, with the maximum value set to 1.0 in each time series. Each data point is the average of two or three independent biological replicates with error bars representing SEM. For each mRNA shown here and in panel D, we tested for a significant difference in expression (one-way ANOVA) across the time series. Significant differences in expression was detected for all transcripts ($p < .05$) except for *per* and *Pka-C3*, which showed differences only between peak and trough by t-test only ($p < .005$ for *per* and $p < .01$ for *Pka-C3*).

(D) Real-time qPCR curves as in C for five additional enriched clock-driven genes: *Pka-C3* (blue diamonds), *CG14251* (orange squares), *CG14853* (green triangles), *CG33275* (red squares) and *CG44238* (black squares).

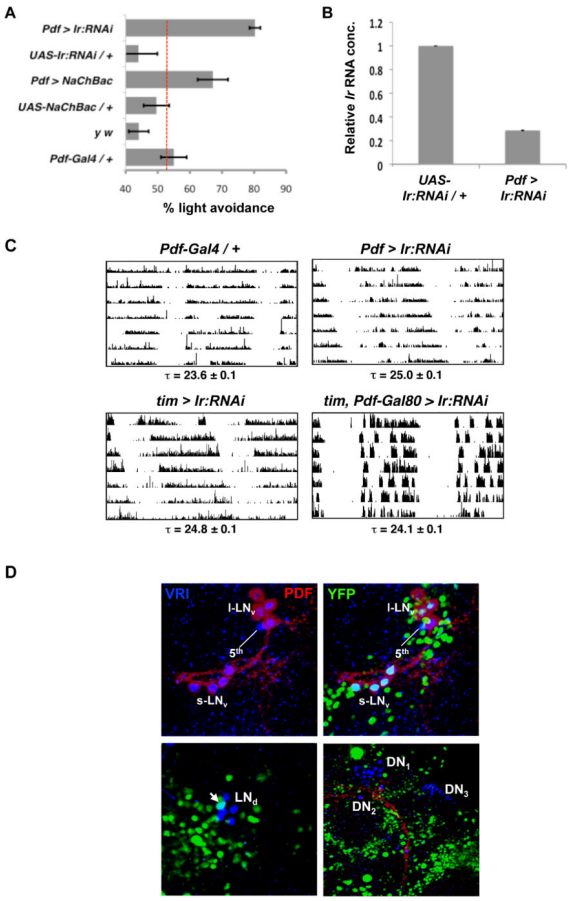

Figure 3. Reduced *Ir* levels in LN_vs affect larval and adult behavior

(A) Foraging 3rd instar larvae were tested for avoidance of the light half (30 lux) of a Petri dish. The percentage of larvae on the dark side of the dish after 15 min is shown as a measure of light avoidance. Control *y w*, *UAS-NaChBac/+* and UAS-*Ir:RNAi/+* larvae do not avoid light at this intensity and are not significantly different from each other (p>0.1 for all comparisons, t-test). Red dotted line indicates 50% light avoidance i.e. when larvae cannot differentiate between 30lux light and darkness. Larvae with the *Pdf-Gal4* driver and either *UAS-NaChBac2* (*Pdf > NaChBac*) or UAS-*Ir:RNAi* (*Pdf > Ir:RNAi*) avoid light significantly better than the three control strains (p<.01). These experiments were performed between ZT 14 and ZT 16. Bars show averages of 12 plates each with ~15 larvae in each plate. Error bars show SEM.

(B) Real-time qPCR on amplified LN_v RNA from either control larvae (*UAS-Ir:RNAi*/+) or with *Pdf-Gal4* expressing *UAS-Ir:RNAi* (*Pdf > Ir:RNAi*) at ZT15. RNA levels were normalized to noncycling levels of *Pdf*, with the maximum value set to 1.0. *Ir* RNA levels are lower in *Pdf > Ir:RNAi* than in control LN_vs ($p < 0.0005$, t-test). Data are the average of two independent experiments. Error bars show SEM.

(C) Actograms showing adult locomotor activity in DD. Top panels: *Pdf-Gal4/+* controls have a shorter period than flies with *Pdf-Gal4* expressing *UAS-Ir:RNAi* (*Pdf > Ir:RNAi*, $p < .01$). *Pdf > Ir:RNAi* flies also have longer periods than flies with *Pdf-Gal4* expressing a control RNAi ($p < .01$, Table S4). Bottom panels: Flies with *tim-UAS-Gal4* expressing *UAS-*

Ir:RNAi in all clock neurons (*tim > Ir:RNAi*) have longer periods than the *tim-UAS-Gal4, Pdf-Gal80* combination expressing *UAS-Ir:RNAi* in all clock neurons except LN_vs (*tim, Pdf-Gal80 > Ir:RNAi*, $p < .01$) or control *tim-UAS-Gal4/+* or *UAS-Ir:RNAi/+* flies ($p < 0.01$, Table S4). Period (chi-squared analysis) and SEM are reported for flies with significant activity rhythms.

(D) Immuno-stainings with UAS-nuclear-YFP (Kimura, 2005) reporting expression from the *Ir-Gal4* enhancer trap. Adult brains were dissected at ZT15 and stained using antibodies to GFP (to detect YFP, green), PDF (to mark LN_vs, red) and VRI (to mark all clock neurons, blue). Top panels show LN_vs. Nuclear YFP was detected in all four PDF+ s-LN_vs in all 10 brains examined, in 2–3 of the 5 l-LN_vs but never in the 5th PDF- s-LN_v. YFP was detected in 1 of the 6 dorsal Lateral Neurons (LN_ds, lower left panel), but not in any dorsal neuron groups (DN_1, DN_2 or DN_3, lower right panel).

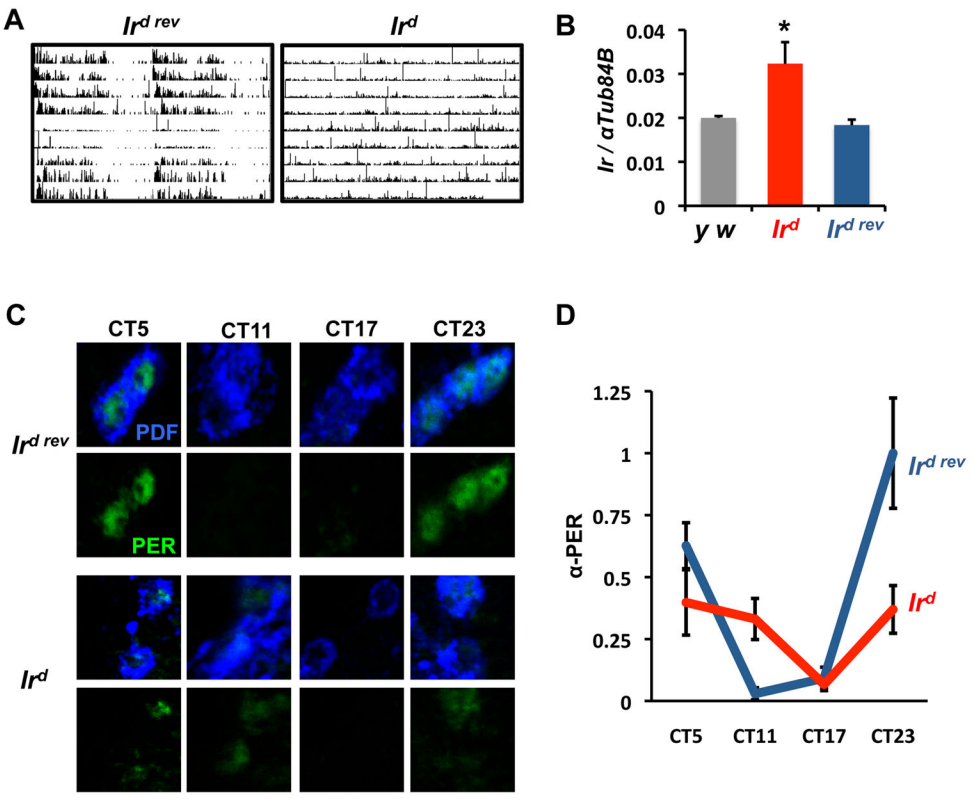

Figure 4. Increasing *Ir* expression disrupts adult circadian behavioral and molecular rhythms

(A) A P-element inserted in *Ir* (Ir^d) makes ~50% of flies lose behavioral rhythms and this phenotype is rescued by excision of the P element ($Ir^{d\ rev}$).

(B) *Ir* RNA levels in RNA isolated from whole fly heads are higher in Ir^d flies than in *y w* or $Ir^{d\ rev}$ control flies ($p < 0.05$, t-test). The data are an average of 4 biological replicates isolated at ZT11. Error bars show SEM.

(C) Representative images of PER protein levels in adult s-LN_vs of $Ir^{d\ rev}$ control flies (top panels) and Ir^d flies (bottom panels) at 4 time points on the 5th day in DD. The locomotor activity of the flies stained here was not assayed and so the Ir^d flies are likely a mix of rhythmic and arrhythmic animals.

(D) Quantitation of data from C normalized to peak PER levels at CT23 in $Ir^{d\ rev}$ controls. Error bars show SEM. PER levels are lower at CT23 in Ir^d (red) than in $Ir^{d\ rev}$ s-LN_vs (blue, $p < 0.05$, t-test).